



He effects in concentrated equiatomic
refractory alloys with increasing
chemical complexity:
From medium to high entropy alloys
(HerHEA)

EUROFUSION ENR-MAT.02.VTT-T001

01/01/2024 → 31/12/2025

PI: Prof. Flyura Djurabekova



Partners of the HeRHEA project

- VTT:

- Prof. Flyura Djurabekova (UHEL) – PI of HerHEA project
- Prof. Filip Tuomisto (UHEL)
- Dr Kenichiro Mizohata (UHEL)
- Dr. Jesper Byggmästar (UHEL)
- Dr. Guanying Wei (UHEL)
- MSc Zhehao Chen (UHEL)
- BSc Toni Sutinen (UHEL)
- Dr Tomi Suhonen (VTT)
- Dr. Goel Sneha (VTT)

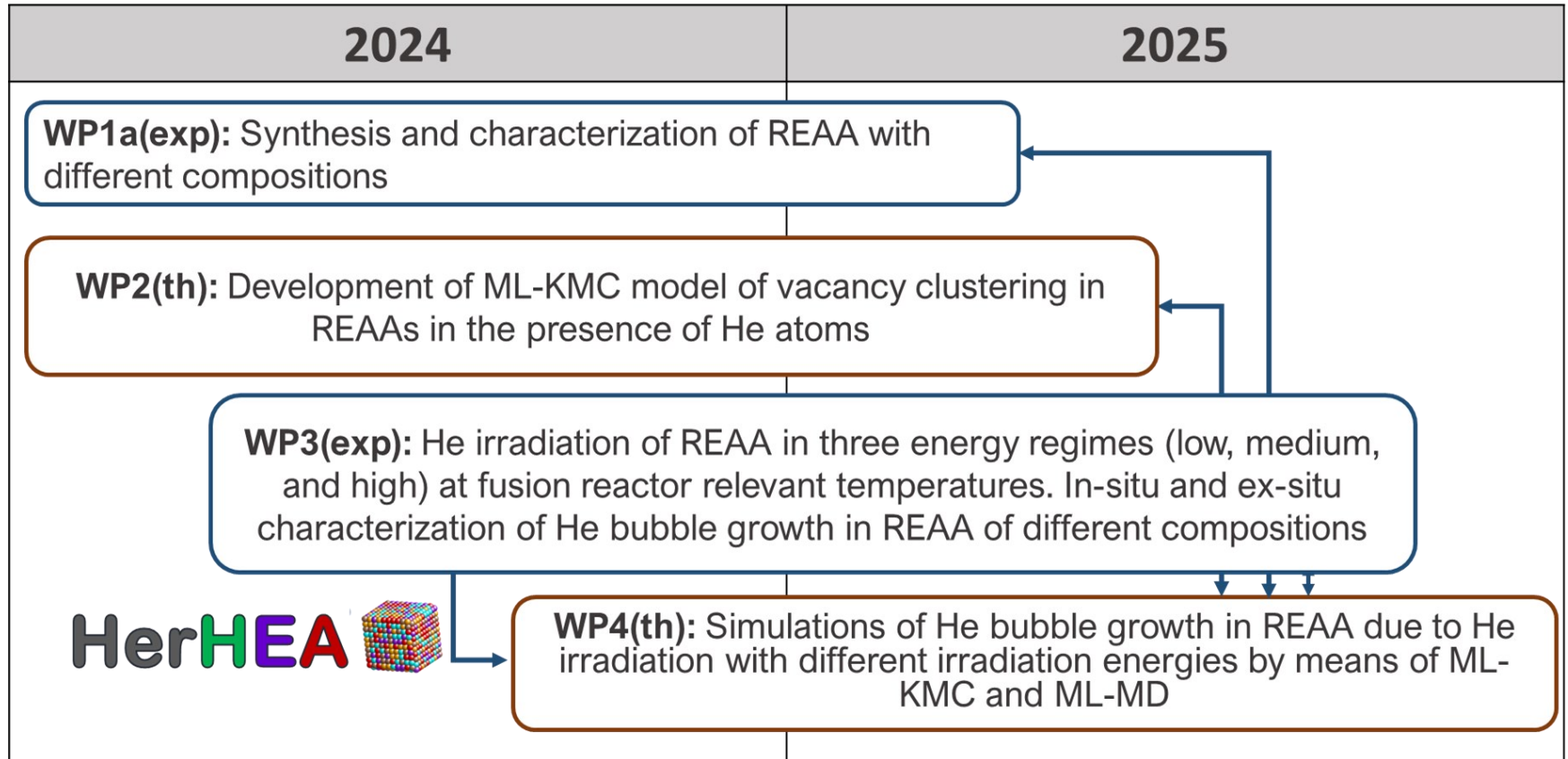
- CEA:

- Prof. Marie-France Barthe
- Dr. Pierre Desgargin
- Dr. Thierry Sauvage
- Dr. Z Hu
- Dr. J. Joseph
- Dr. O. Wendling
- Dr. F. Foucher
- Dr. C. Genevois
- Dr. Aurélie Gentils
- Dr. Stéphanie Jublot-Leclerc
- Dr. Antoine Combrisson





Timeline of HeRHEA project





WP2(th) “Development of ML-KMC model of vacancy clustering in REAAs in the presence of He atoms”

The diffusion of He in W-based refractory alloys by molecular dynamics



Potential He-refractory alloys

$$f(r_{ij}) = \begin{cases} \text{ZBL}, & r_{ij} \leq r_1, \\ e^{b_0 + b_1 r_{ij} + b_2 r_{ij}^2 + b_3 r_{ij}^3}, & r_1 \leq r_{ij} \leq r_2, \\ \sum_{n=1}^{12} a_n (r_n - r_{ij})^3 H(r_n - r_{ij}), & r_{ij} \geq r_2, \end{cases} \quad (1)$$

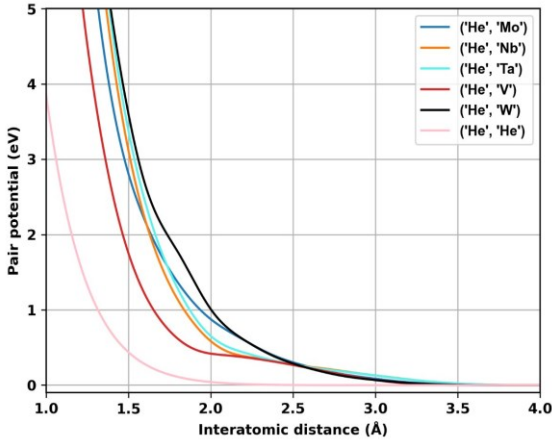


Table 2: Properties used for fitting and testing the interaction between refractory metals and He. Tetra. and Octa. means the formation energy of a He at the tetrahedral and octahedral positions. E_{binding} means the binding energy between an interstitial He with a vacancy. E_{mig} means the migration energy of He. Reference values are from the corresponding DFT, ab-initio and MD calculations. All the units are eV.

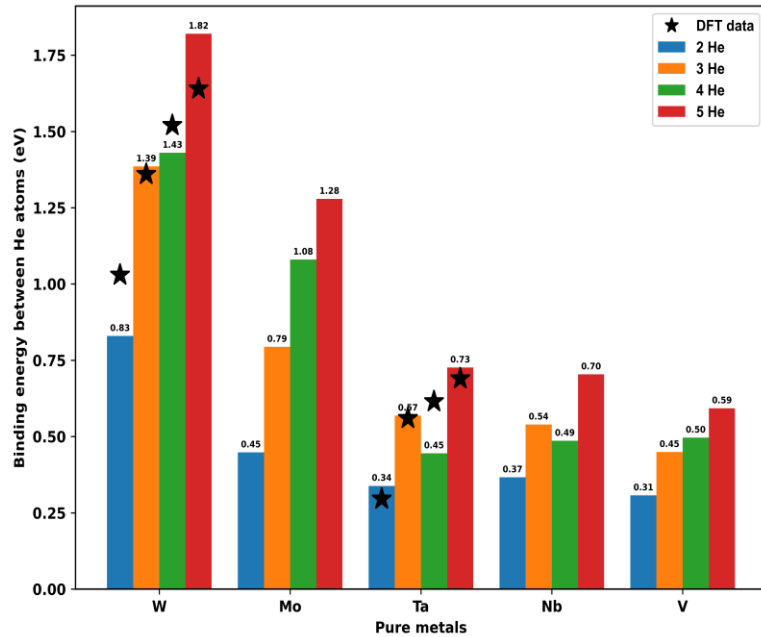
W-He	Present value	Reference values	Mo-He	Present value	Reference values
Tetra.	6.18	6.15 ^[23] , 6.16 ^[118] , 6.22 ^[24, 16] , 6.23 ^[26]	Tetra.	5.33	5.16 ^[27] , 5.28 ^[28] , 5.31 ^[18] , 5.33 ^[29]
Octa.	6.34	6.31 ^[18] , 6.34 ^[16] , 6.37 ^[4, 24] , 6.38 ^[4] , 6.44 ^[25] , 6.48 ^[26]	Octa.	5.44	5.33 ^[27] , 5.45 ^[28] , 5.48 ^[29] , 5.49 ^[18]
E_{binding}	4.76	4.57 ^[4, 1] , 4.62 ^[26] , 4.63 ^[25] , 4.75 ^[18] , 4.91 ^[16]	E_{binding}	3.65	3.64 ^[28] , 3.65 ^[18] , 3.66 ^[29] , 3.67 ^[27]
E_{mig}	0.09	0.06 ^[4, 118] , 0.07 ^[23, 26] , 0.09 ^[16]	E_{mig}	0.09	0.06 ^[18]
Ta-He	Present value	Reference values	Nb-He	Present value	Reference values
Tetra.	3.46	3.16 ^[27] , 3.34 ^[30] , 3.41 ^[31, 24] , 3.45 ^[16] , 3.46 ^[18]	Tetra.	3.18	3.05 ^[27] , 3.13 ^[18]
Octa.	3.59	3.42 ^[27] , 3.60 ^[16] , 3.65 ^[30] , 3.68 ^[24] , 3.74 ^[31] , 3.79 ^[18]	Octa.	3.34	3.26 ^[27] , 3.40 ^[18]
E_{binding}	1.79	1.62 ^[31] , 1.67 ^[32] , 1.79 ^[18] , 1.81 ^[16]	E_{binding}	1.49	1.49 ^[18] , 1.67 ^[27]
E_{mig}	0.09	0.09 ^[30, 118] , 0.10 ^[32] , 0.11 ^[16]	E_{mig}	0.11	0.09 ^[18]
V-He	Present value	Reference values			
Tetra.	3.20	2.94 ^[27] , 3.09 ^[24] , 3.17 ^[18]			
Octa.	3.35	3.17 ^[27] , 3.31 ^[24] , 3.40 ^[18]			
E_{binding}	1.16	0.91 ^[27] , 1.16 ^[18]			
E_{mig}	0.11	0.09 ^[18]			

- We have developed the interatomic potential to describe the interaction of He atoms with all atoms in high-entropy alloy (HEA) composition. The interactions are purely repulsive, the HEA is described by previously developed tab-GAP potential [J. Byggmästar, K. Nordlund, F. Djurabekova, Simple machine-learned interatomic potentials for complex alloys, Phys. Rev. Materials 6 (8) (2022) 083801]
- Table 2 illustrates the comparison of formation, migration and binding energies for He atoms in mono-elemental metals

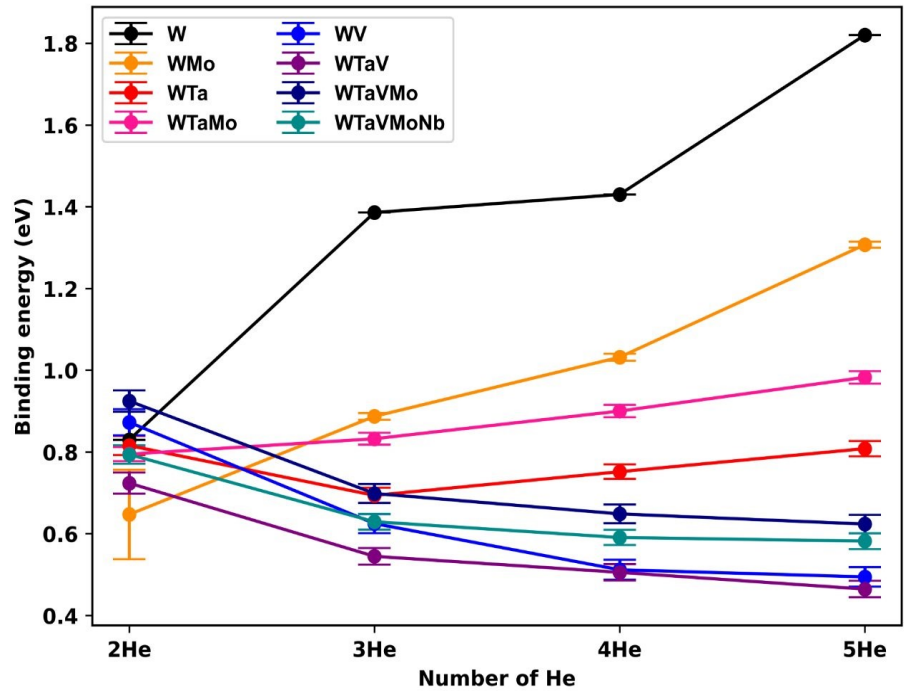


Binding energy between He clusters

Pure metals



W and W-based alloys



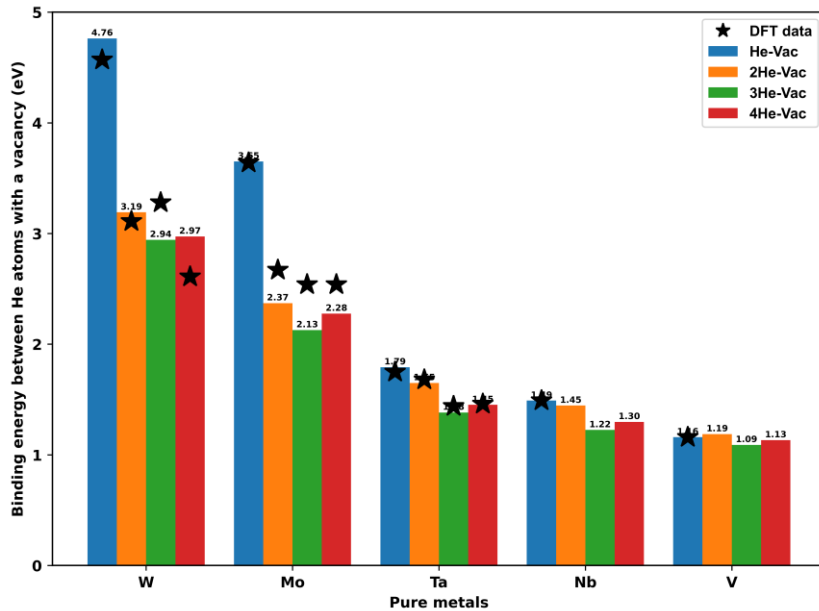
- References for DFT value:
- Ta: You et al, The behaviors of helium atoms in tantalum, rhenium and osmium, Journal of Nuclear Materials, 2018(499).
- W: Becquart et al, An object Kinetic Monte Carlo Simulation of the dynamics of helium and point defects in tungsten, Journal of Nuclear Materials, 2009(385).

$$E_{\text{binding}}(D_1, D_2) = E(D_1) + E(D_2) - E(D_1 + D_2) - E_{\text{ref}}$$

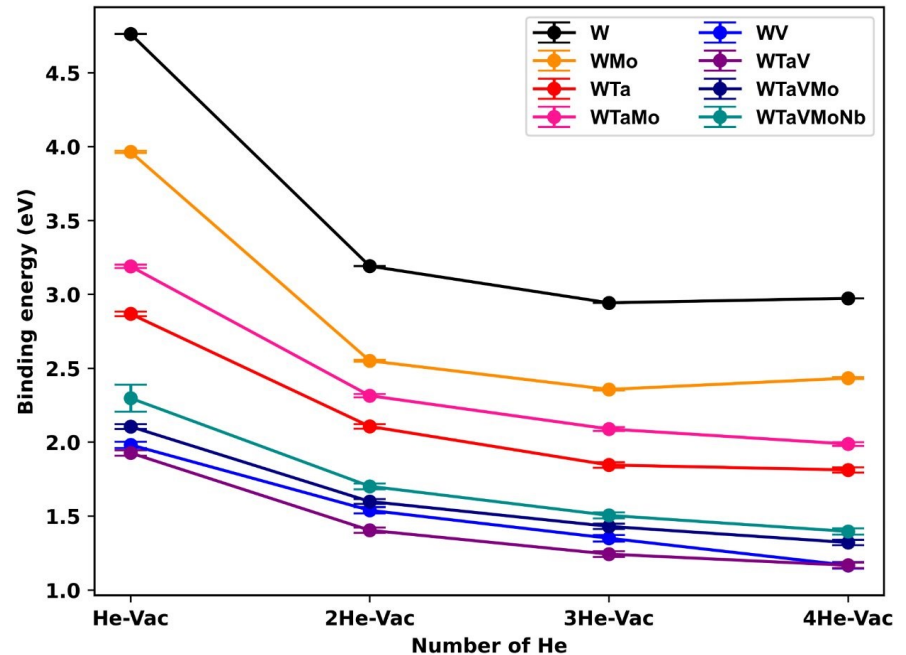


Binding energies of He to vacancy

Pure metals



W and W-based alloys



- References for the DFT values:

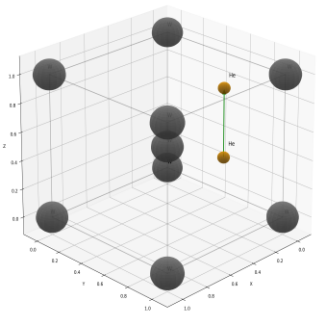
- W: Becquart et al, An object Kinetic Monte Carlo Simulation of the dynamics of helium and point defects in tungsten, Journal of Nuclear Materials, 2009(385).
- Mo: Runnevall et al, Helium cluster dissolution in molybdenum, Journal of Physics: Condensed Matter, 2009(21).
- Ta: Omori et al, First principle calculations of energy of agglomerated helium in the period 6 elements, Nuclear Materials and Energy, 2018(16).
- Nb & V: Jiang et al, Ab initio theory of noble gas atoms in bcc transition metals, Physical Chemistry Chemical Physics, 2018(25).



Average migration energy of a He atom

He position	WMo	WTa	WTaMo	WV	WTaV	WTaVMo	WTaVMoNb
$(0,0.5,0.25)*a$ ↓ $(0,0.5,0.75)*a$ (a : lattice constant)	0.13 ± 0.003	0.20 ± 0.004	0.196 ± 0.008	0.43 ± 0.007	0.34 ± 0.005	0.32 ± 0.005	0.29 ± 0.004

Migration path



Pure metals

Migration energy	Mo	Nb	Ta	V	W
DFT data[1]	0.09	0.11	0.09	0.09	0.06
Our results	0.06	0.09	0.09	0.09	0.06

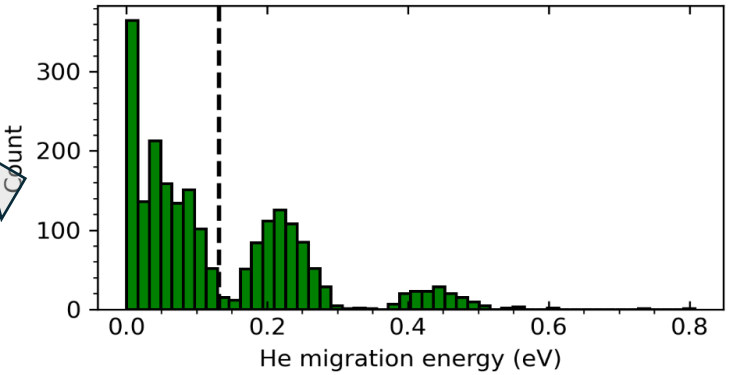
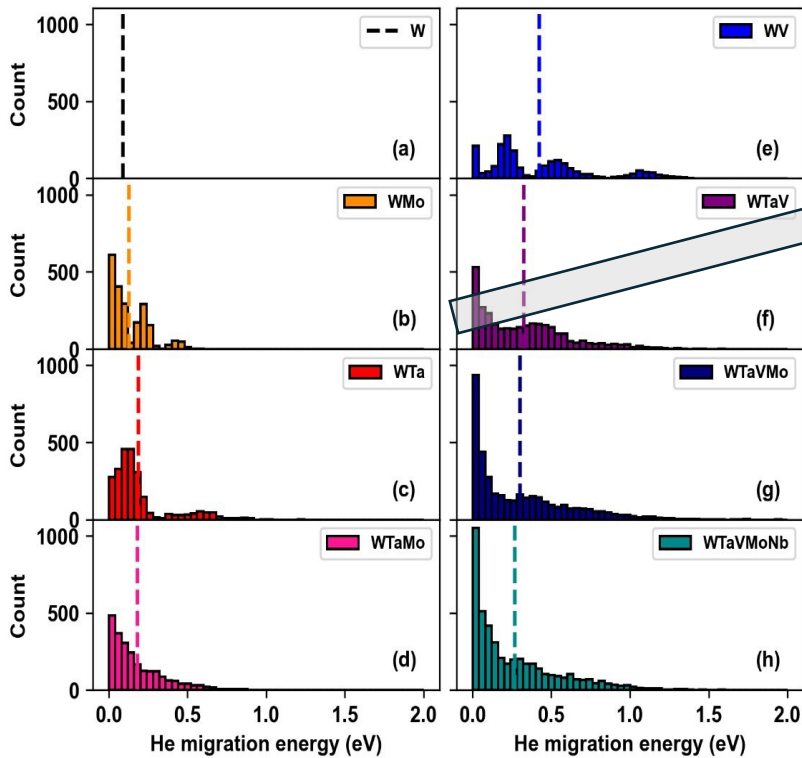
[1]: Jiang et al, Ab initio theory of noble gas atoms in bcc transition metals, Physical Chemistry Chemical Physics, 2018(25).



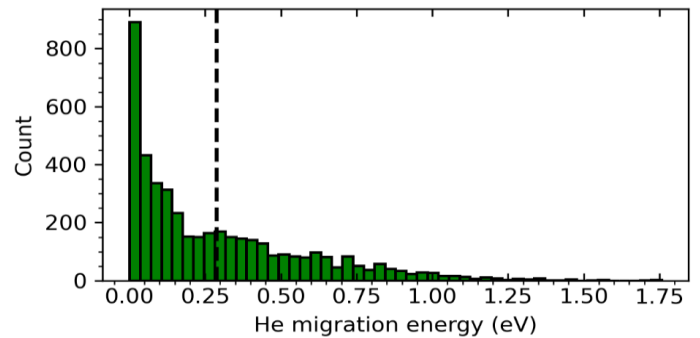
Migration energy of a He atom

NEB results

- The effect of chemical environment on He migration



WMo

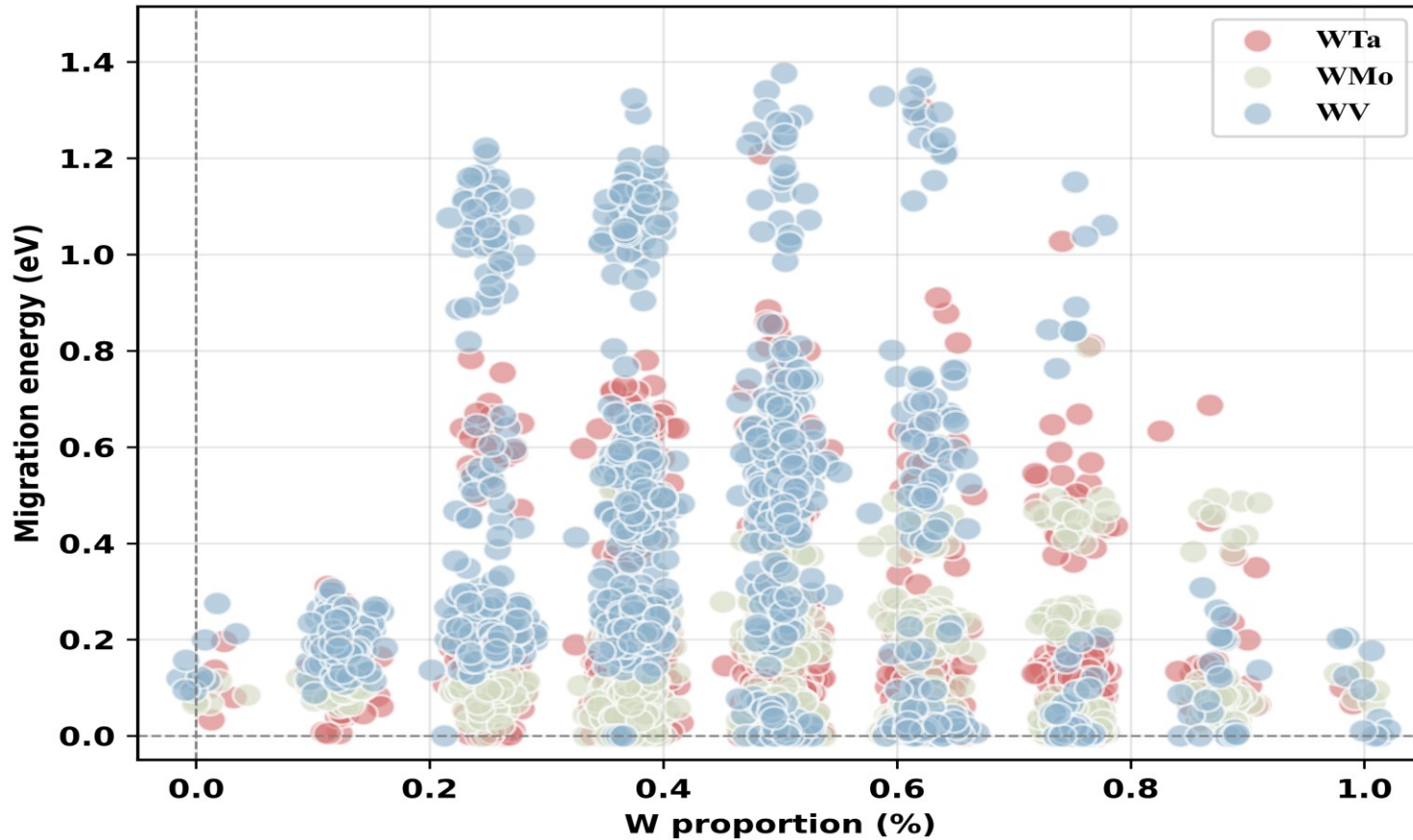


WTaVMoNb

The distribution of migration energies



Migration energy of a He atom

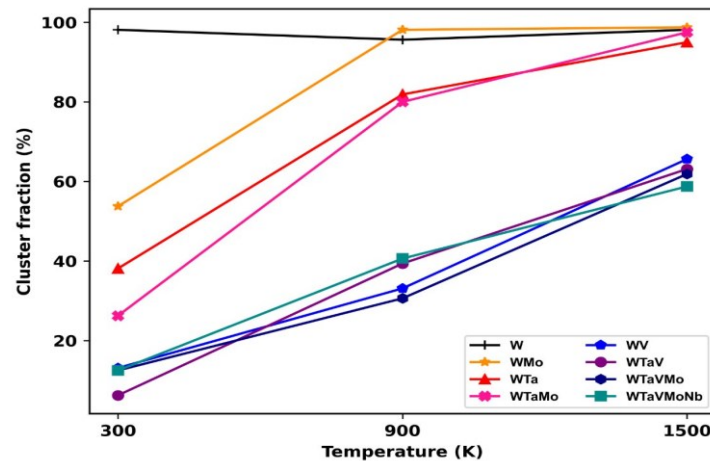


- Effect of W coordination environment on the migration energy of He atoms



Diffusion of He (MD simulation)

- Simulation details:
 - Box size: $20 \times 20 \times 20 = 16000$ atoms with 0.1% Vacancies(16) and 1% He (160 atoms)
 - Relaxation runs in NPT ensemble for 5 ns at 300 K, 900 K and 1500 K



- We observe a strong He clustering in W at all temperatures, while in the V-containing alloys, the growth is much slower. The He atoms prefer to remain dissolved in the lattice



Final frames at all three temperatures for W and WV

300 K

900 K

1500 K

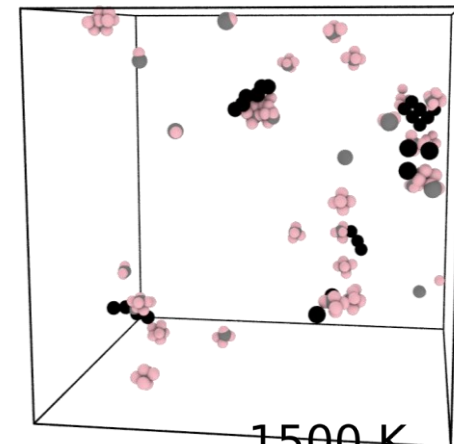
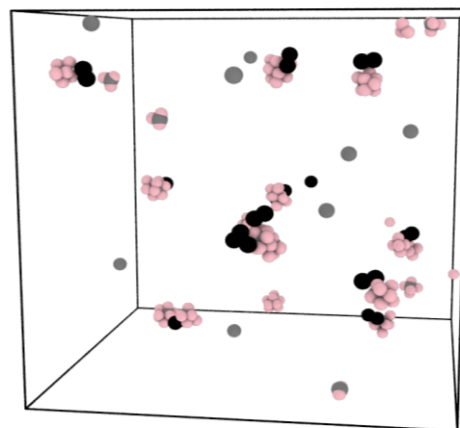
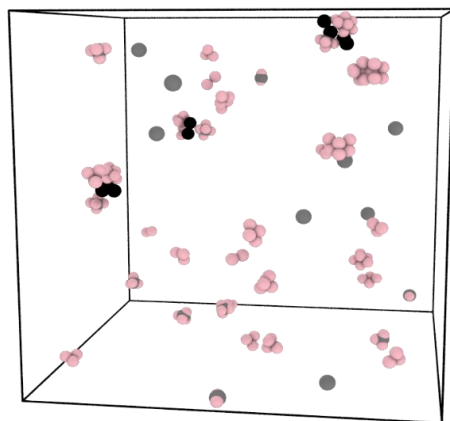
W

Pink: He

Gray: Vacancies

Black: W

interstitials



300 K

900 K

1500 K

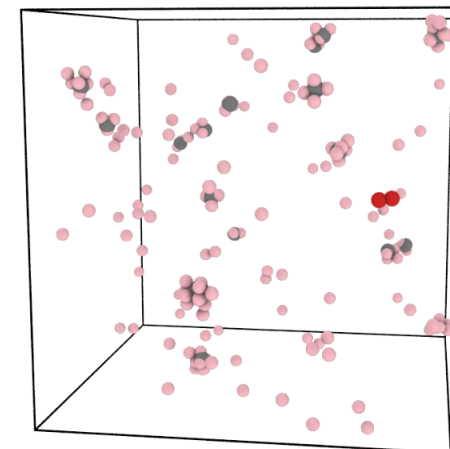
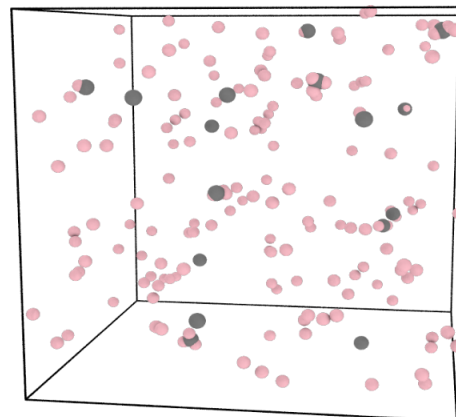
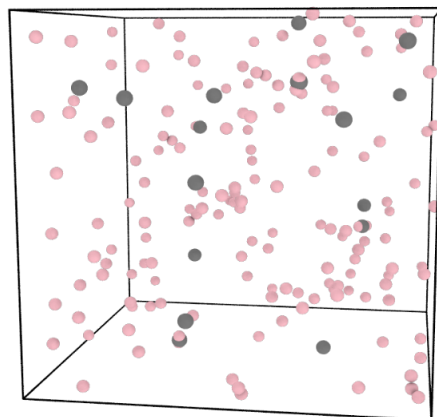
WV

Pink: He

Gray: Vacancy

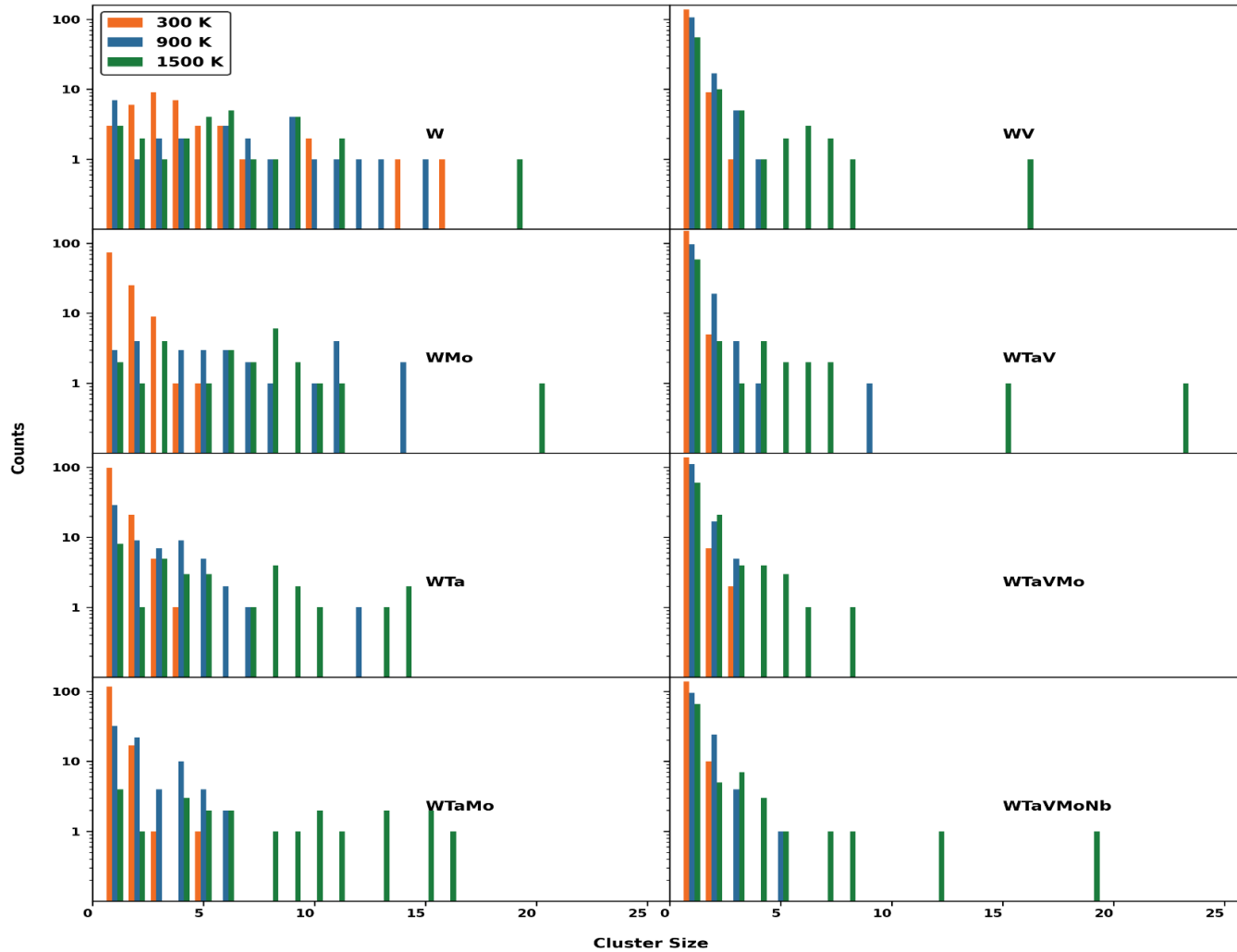
Black: W interstitials

Red: V interstitials





Distributions of He cluster size

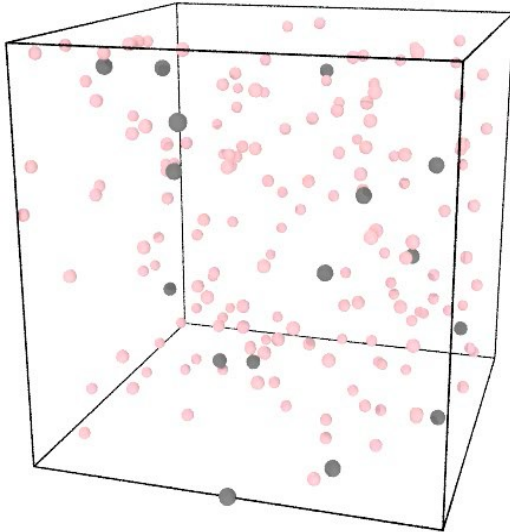
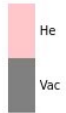




Evolution of diffusion (1500 K)

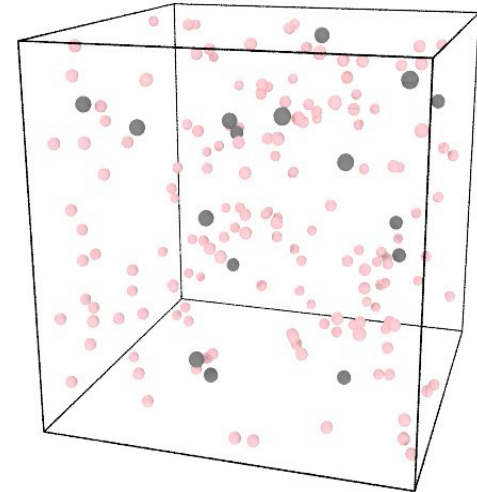
W

Particle types



WV

Particle types



- Dynamic evolution of He clustering at 1500 K in W and WV as an example of V-containing alloy



WP3(exp):

He irradiation of REAA in three energy regimes (low, medium, and high) at fusion reactor relevant temperatures.

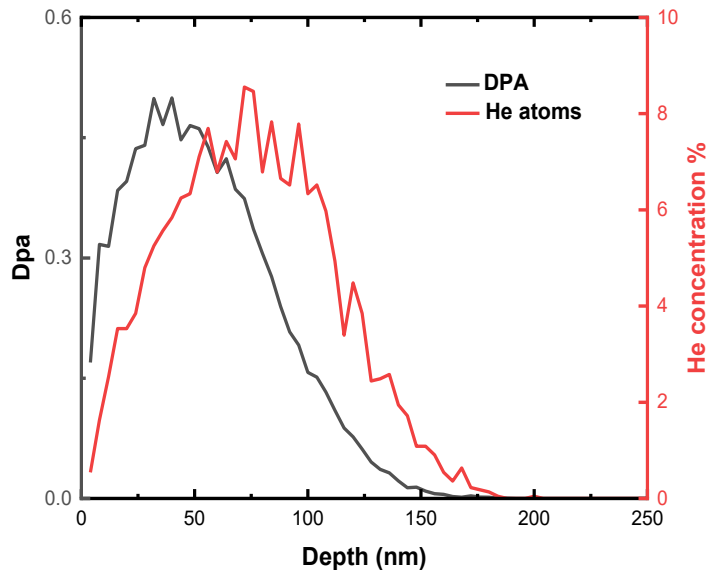
In-situ and ex-situ characterization of He bubble growth in REAA of different compositions

Experimental study: Suppression of long-range helium migration in HEAs

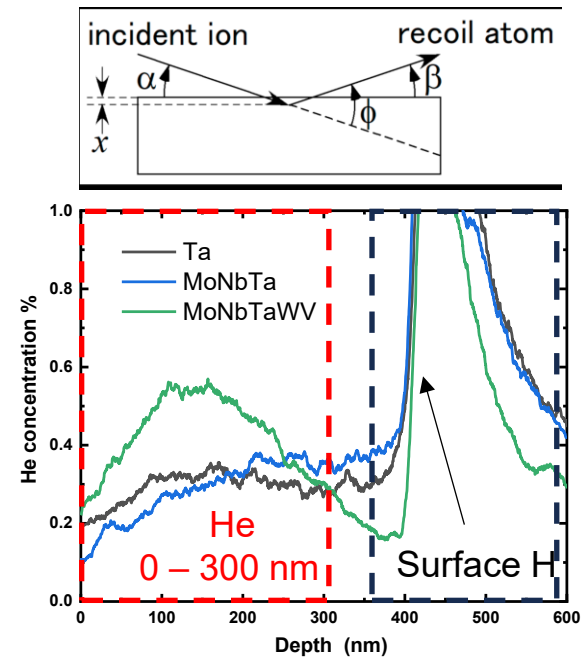


He in Ta series Refractory HEA (BCC) (unpublished)

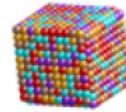
- Samples: Arc-melted Ta, MoNbTa, MoNbTaWV
- Irradiation: 5×10^{16} , 25 keV He (ions/cm²), room temperature (RT)
- Method: Elastic recoil detection (ERDA), direct measurement of helium concentration within 0-300 nm



SRIM simulation of 25 keV He in Ta

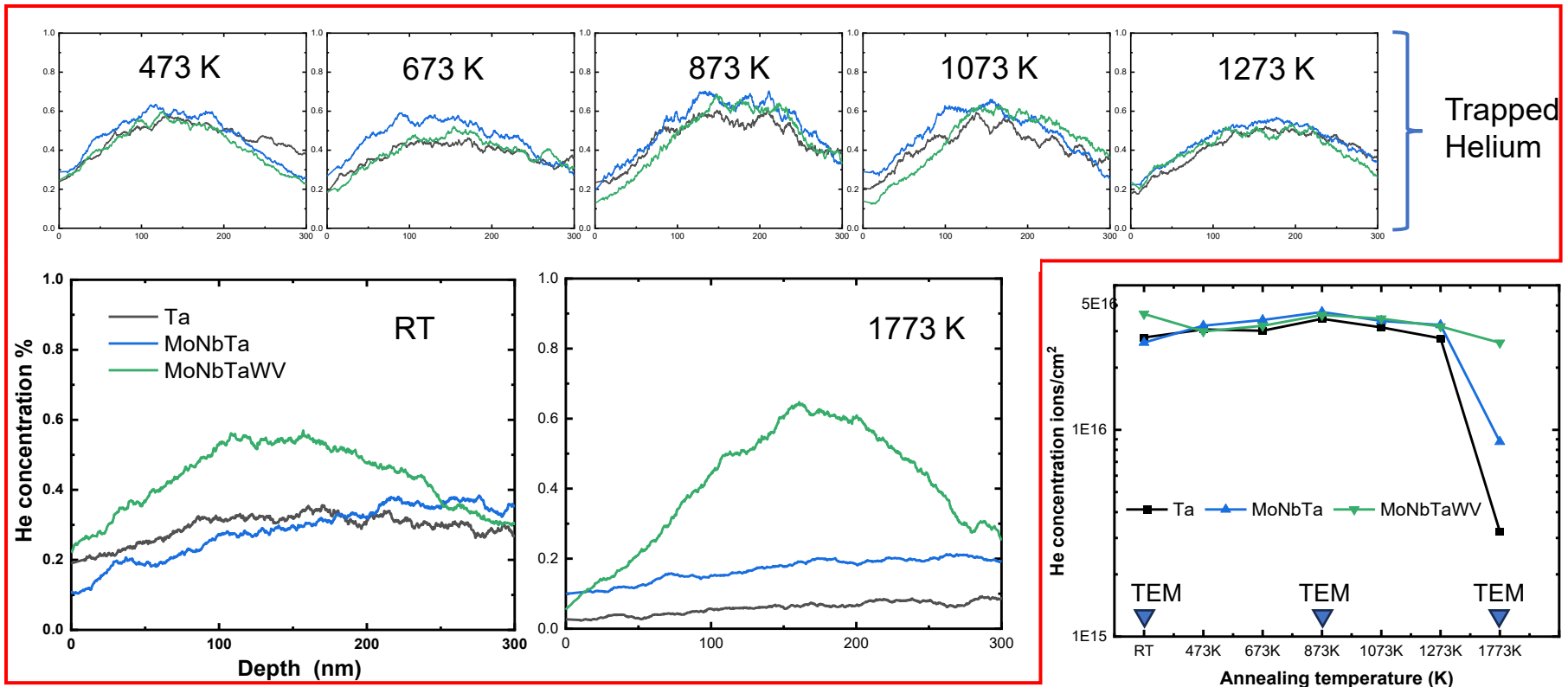


ERDA principle and spectrums after RT irradiation



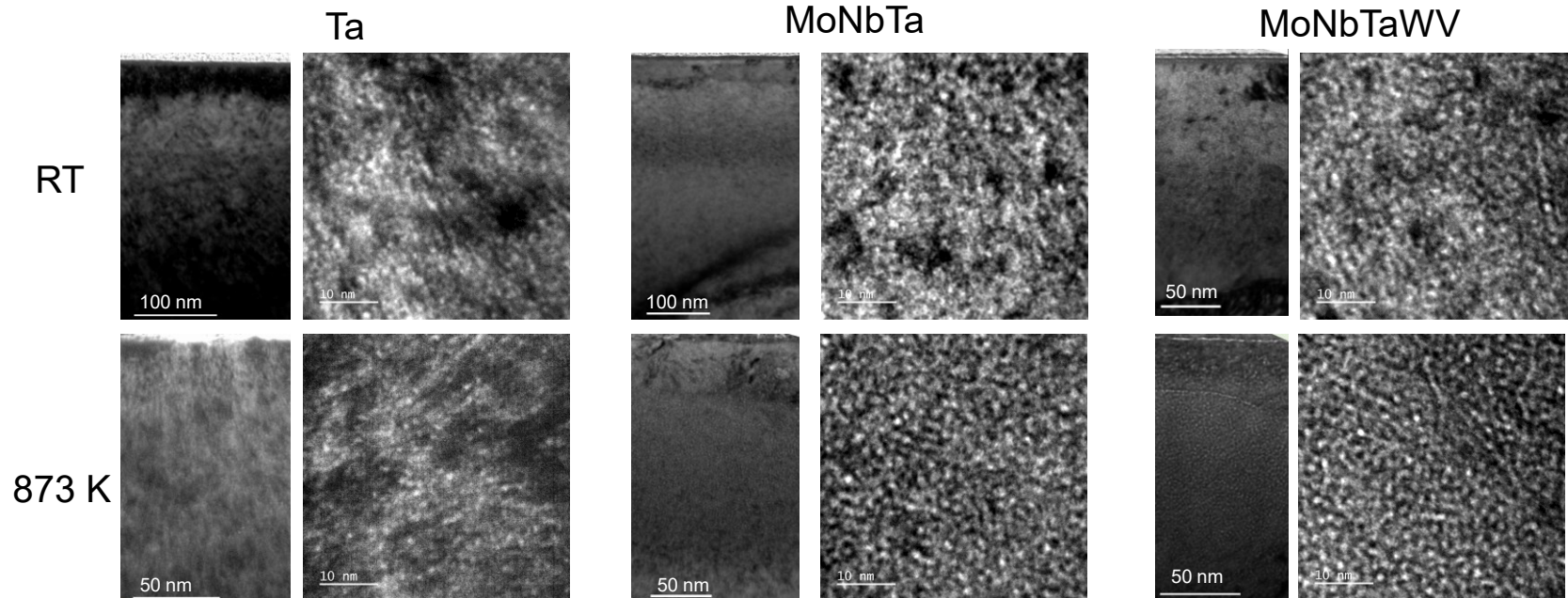
Helium depth profile after annealing at RT -1773 K for 1h

- For reference, $0.5T_m$: Ta ~1645 K, MoNbTa ~1490 K, MoNbTaWV ~1482 K





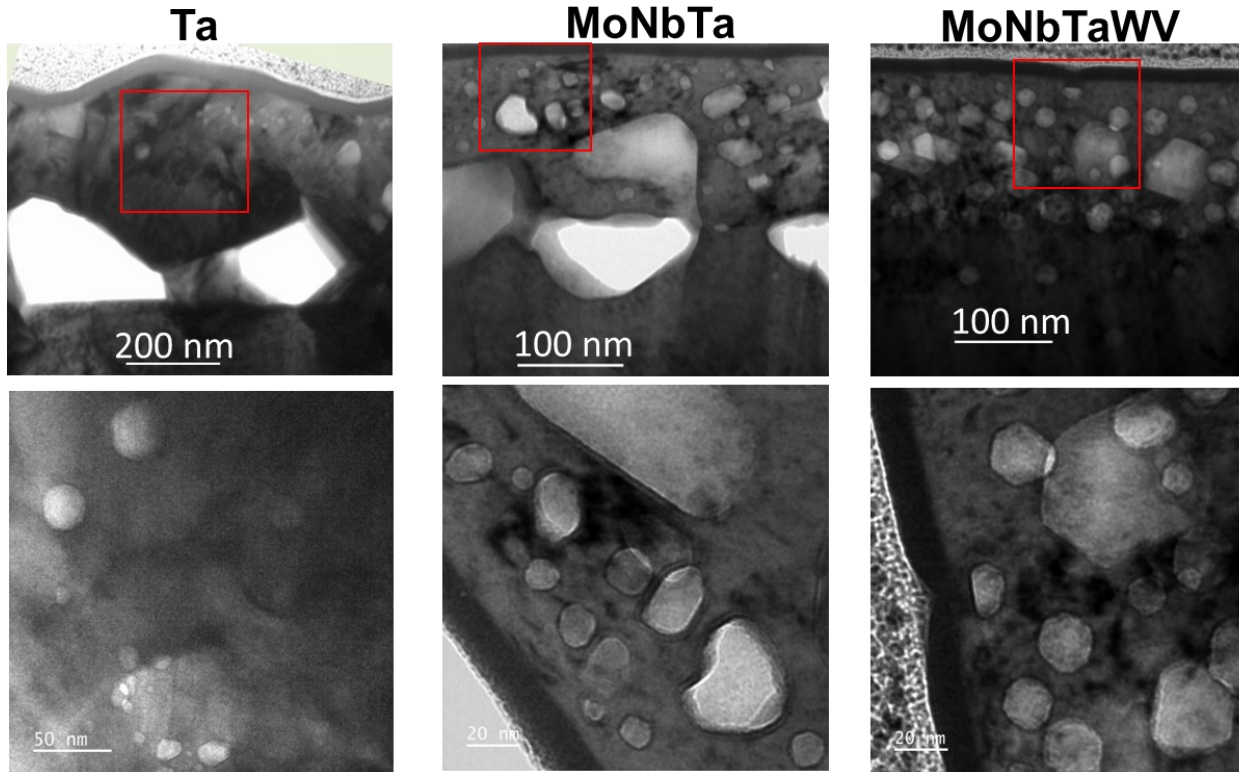
Helium Cavities: at RT and 873 K



- The damage peak is located at a depth of approximately 200 nm
- Helium cavities size: 1-2 nm
- No significant changes were observed between the measurements at room temperature to 873 K.



Helium Cavities: at 1773 K

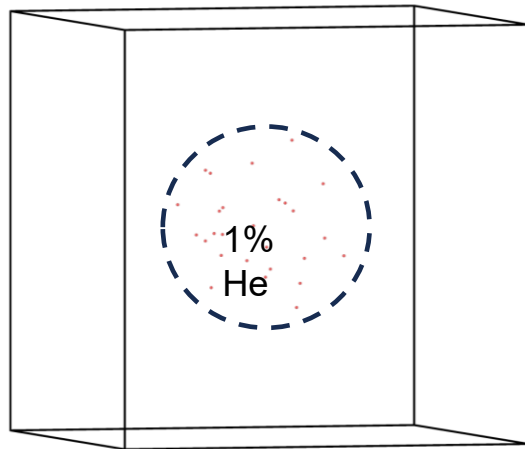


- Helium cavities exhibited significant growth in all samples after reaching half of the melting temperature.
- Less large helium cavities were observed at grain boundaries as the number of principal elements increased, indicating that long-range helium migration was limited.
- In pure Ta, the sample surface was deformed by large cavities.

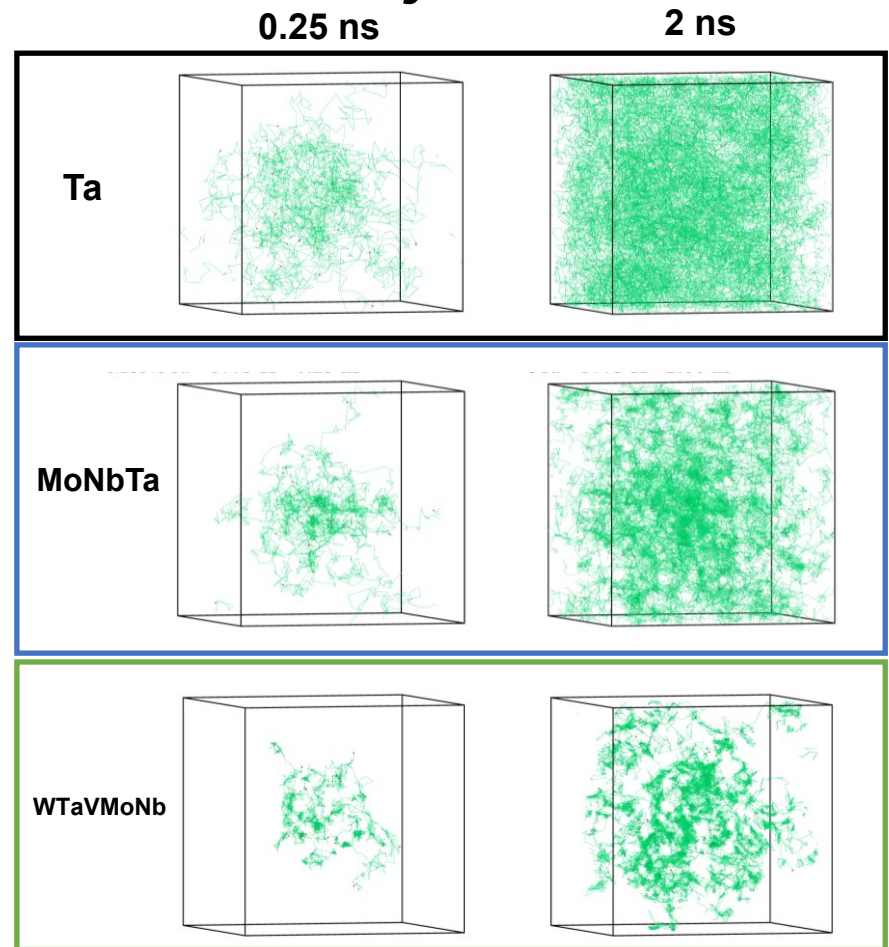


Molecular Dynamics simulation of He diffusion in Ta-based alloys

- Modeling parameters:
- Box size : $30 \times 30 \times 30$, (54000 atoms)
- Central spherical volume : $0.05 \times$ box volume (~2700 atoms), where we Insert 1% He atoms (27 atoms)



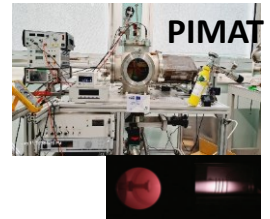
- He atom
- Diffusion path of helium atom





The approach and some first results

- At CEMHTI
 - Preparation of samples (polishing, annealing and preliminary characterization)
 - Two types of He exposure at RT and 500°C
 - Low energy (100-500 eV) using plasma reactor (**PIMAT**) closer to divertor conditions
 - Medium energy (500 keV) using Pelletron accelerator closer to “fast ions” escaping the fusion plasma + α particles (transmutation)
 - Characterization using
 - Nuclear Reaction Analysis (NRA) using deuteron beam and the ^2H (^3He , ^4He) ^1H reaction for He inventory.
 - Positron annihilation spectroscopy (PAS, Doppler broadening spectrometer coupled to a slow positron beam- DBS-SPB) and *ex situ* transmission electron microscopy (TEM) -in some specific samples- for microstructure defects and bubbles
 - Atomic Force Microscopy (AFM) for surface topography
 - Samples : pure W and REAA alloys (arc-melted W-Ta, W-Mo and W-V binaries and ternaries) massive samples prepared by VTT



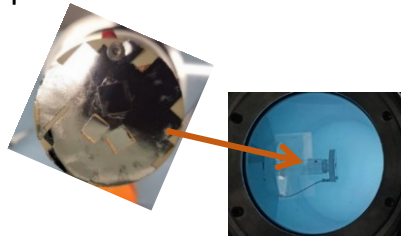


PIMAT : Plasma Irradiation in Materials

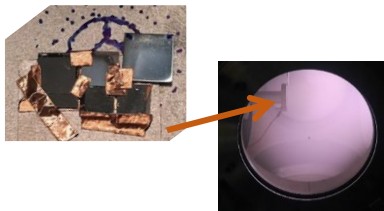
- ^3He exposure in PIMAT

(300 eV)

Flux estimated for homogeneous plasma $\sim 8 \times 10^{15} \text{ m}^{-2} \cdot \text{s}^{-1}$

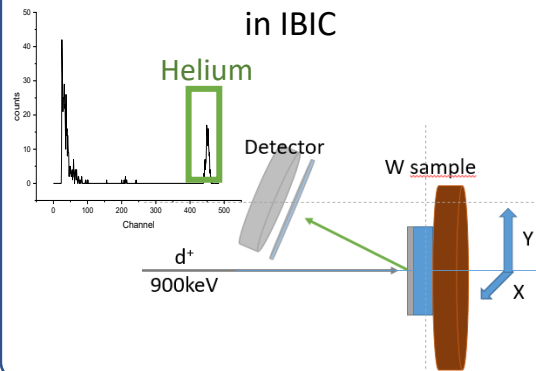


(100) W Single crystal
+ W polycrystals (polished & annealed)

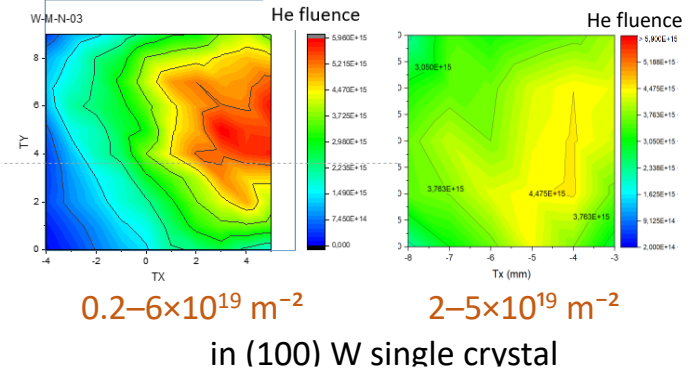


(100) W Single cristal (pol. & ann.) +
W based REA thin layers W, WV & WNbV

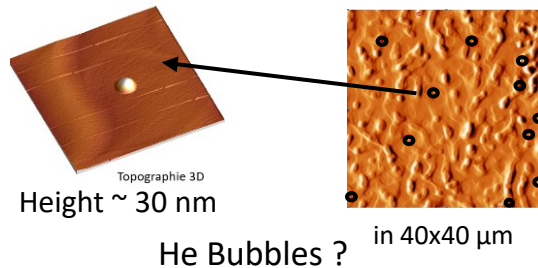
^3He mapping
(NRA, ^2H (^3He , ^4He) ^1H)
in IBIC



Optimisation of plasma conditions
Before & After



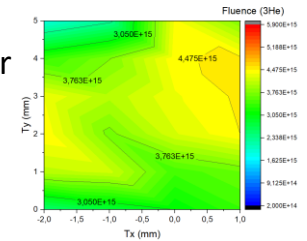
AFM in (100) W single crystal
after exposure $\sim 4 \times 10^{19} \text{ m}^{-2}$



Comparison between W single crystal
and REA thin layers : first results

In W epitaxial layer

$2-5 \times 10^{19} \text{ m}^{-2}$





Work plan

- Initial work plan for 2024

No	Description	Expected date
M1.1	1st generation (batch) of binary alloys samples, incl. basic charac. (WP1)	June 2024
M2.1	Extension of ML-IAP to include He interactions with HEA is ready (WP2)	May 2024
M3.1	He irradiation and implantation profiles (WP3)	Sep 2024
M3.2	High energy He ion irradiation of HEA (1st batch) (WP3)	Dec 2024
M2.2	ML-KMC model for vacancy migration in REAA with different composition including vacancy clusters is ready (WP2)). Links to D2.1	July 2024
M4.1	ML-MD simulations of plastic deformations around He nanobubbles in binary (WTa, WMo, WV)). Links to D4.1	Oct 2024
M2.3	Cascade simulations with recoils from high energy He irradiation to deduce the vacancy cluster size distribution in REAAs with increasing complexity are completed (WP2). Links to D2.1	Dec 2024

- Delivery of samples from VTT was postponed to 2025
- In the meantime in 2024
- Optimisation of Exposure conditions in PIMAT
- Modification of the NRA configuration for He mapping
- Tests of ^3He exposure in W and in W, WV and WNbV thin layers epitaxially grown on MgO substrates (11-20/12/2024)
- Work plan for 2025
- Reception of VTT samples (next week)
- Cutting of samples and preparation
- Preliminary characterizations
- He introduction
- Characterizations NRA, PAS, ex-situ TEM, AFM



Observing the bubbles nucleation and growth by *in situ* ion TEM at IJCLab

- The tasks completed in 2024 :
 - Thin foil preparation dev. / optimization
 - ✓ Literature review
 - ✓ Waiting for the materials (1st test will be done by FIB)
- Preliminary choice of ions parameters (comparable with ex situ experiments + using results obtained by simulation)
 - Helium, 10 to 20 keV, up to the maximum fluence in one day
 - Temperature : RT and 500°C



JANUS
Orsay

mosaic

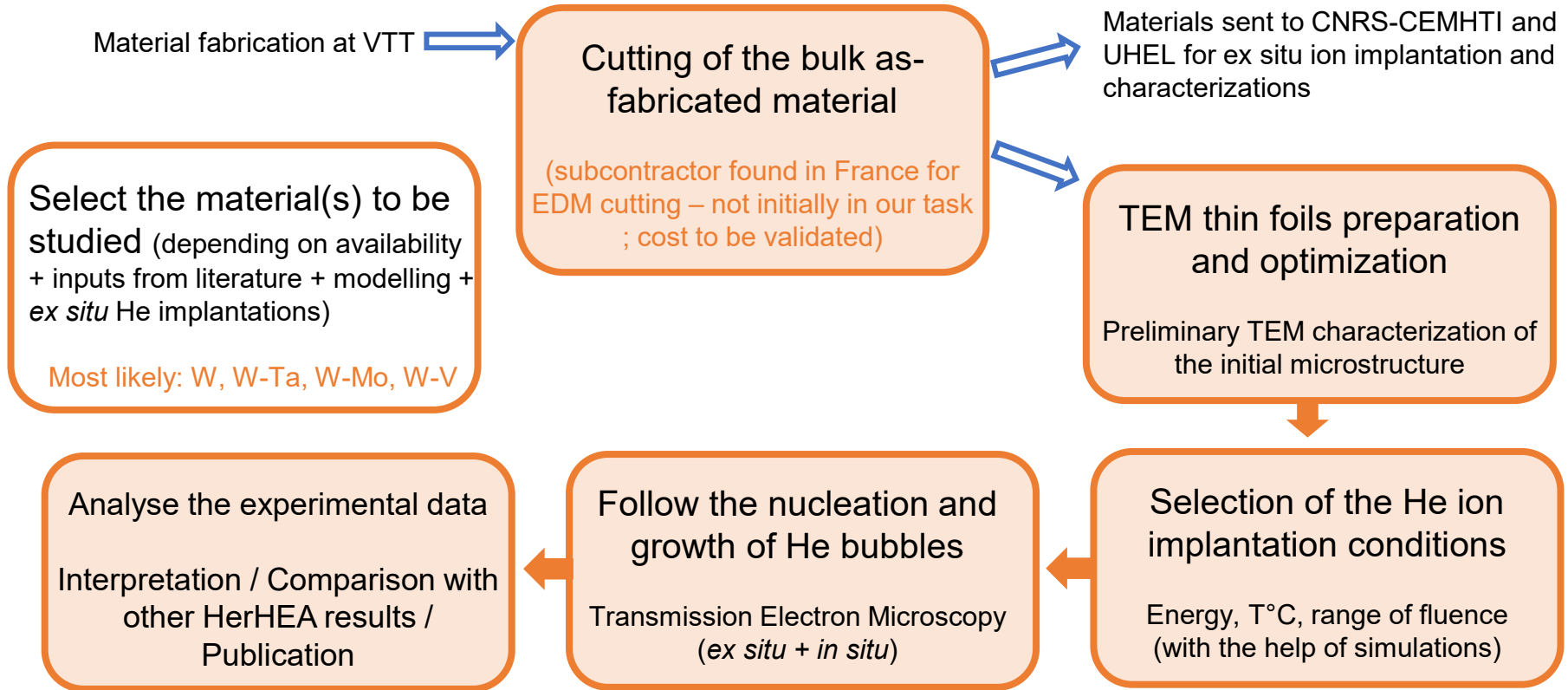
<https://mosaic.ijclab.in2p3.fr>



In situ TEM coupled to 190 kV IRMA ion implanter and 2 MV ARAMIS accelerator



Future work



M3.1 *In situ* TEM experiments performed (Links to D3.1) June 2025 → may be delayed to October



Current published results

- G. Wei, J. Byggmästar, J. Cui., K. Nordlund, J. Ren, F. Djurabekova, Revealing the critical role of vanadium in radiation damage of tungsten-based alloys, V. 274, (1) 2024, 119991; doi.org/10.1016/j.actamat.2024.119991
- Zh. Chen, E. Lu, K. Mizohata, A. Liski, Xu. An, T. Suhonen, A. Laukkanen, J. Lagerbom, A. Pasanen, A. Vaajoki, F. Tuomisto Journal of Nuclear Materials, V. 599, 2024, 155238; doi.org/10.1016/j.jnucmat.2024.155238
- G. Wei, J. Byggmästar, F. Djurabekova, Diffusion of helium in tungsten-based refractory alloys by molecular dynamics, in preparation



Milestones and deliverables

No	Description	Expected date				
M1.1	1st generation (batch) of binary alloys samples, incl. basic charac. (WP1)	June 2024				
M2.1	Extension of ML-IAP to include He interactions with HEA is ready (WP2)	May 2024				
M3.1	He irradiation and implantation profiles (WP3)	Sep 2024				
M3.2	High energy He ion irradiation of HEA (1st batch) (WP3)	Dec 2024				
M2.2	ML-KMC model for vacancy migration in REAA with different composition including vacancy clusters is ready (WP2)). Links to D2.1	July 2024				
M4.1	ML-MD simulations of plastic deformations around He nanobubbles in binary (WTa, WMo, WV)). Links to D4.1	Oct 2024				
M2.3	Cascade simulations with recoils from high energy He irradiation to deduce the vacancy cluster size distribution in REAAs with increasing complexity are completed (WP2). Links to D2.1	Dec 2024				
M3.1	He irradiation and implantation profiles, 2nd batch damage build up (WP3)	Sep 2025				
M1.5	2nd generation (batch) of ternary WTaV and basic characterisation (WP1). Links to D1.3					
M4.2	Analysis of He self-trapping mechanism in R					
M3.1	<i>In situ</i> TEM experiments performed (Links to					
M4.3	ML-KMC model for migration of vacancies He atoms in REAA with different composition ready (WP2). Links to D2.1					
M4.4	ML-MD simulations of plastic deformations in WTaV alloy and RHEA WTaMoNbV (WP4					
			Title	WP	Due date	Description
			D1.1	WP1	Sep 2024	Report on 1 st batch sample synthesis and mechanical properties characterization
			D1.3	WP1	June 2025	Report on 2 nd batch sample synthesis and characterization
			D2.1	WP2	Jan 2025	Report and submitted publication on parameterization of the KMC model for vacancy diffusion with and without He load
			D4.1	WP4	Oct 2025	Report and submitted publications on possible He bubble growth via plastic deformations in REAA with increased complexity
			D3.1	WP3	Dec 2025	Report and submitted publication on <i>in situ</i> TEM analysis of He bubbles
			D4.2	WP4	Dec 2025	Report and submitted publication on He bubble growth via vacancy clustering and agglomeration of vacancy clusters
			DD	All	Jan 2026	Submission of materials data to Eurofusion materials database (foreseen to be in one of ETASC Advanced Computing Hubs).
			DF	All	Jan 2026	Final report on project including outlook for further work.



Outlook for 2025

- In 2025 we will focus on WP4, where the KMC model to describe the bubble agglomeration in V-containing HEA will be developed
- Meanwhile, we will investigate the He bubble growth mechanisms in several alloys (ongoing work)
- Initial experimental results agree with the experimental observations, clearly showing more localized diffusion of He in V-containing concentrated alloys
- While the sample preparation appears to be an issue (some bureaucratic delay at VTT-VTT site with opening of the project), we are looking for other sources of HEA.
- As risk mitigation, we will explore the thin-film grown alloys, which will help us to reveal the effect of chemical composition on He self-trapping and long-range migration